

See discussions, stats, and author profiles for this publication at: <https://www.researchgate.net/publication/7952374>

Substituent Effects on the Edge-to-Face Aromatic Interactions

ARTICLE *in* JOURNAL OF THE AMERICAN CHEMICAL SOCIETY · APRIL 2005

Impact Factor: 12.11 · DOI: 10.1021/ja037454r · Source: PubMed

CITATIONS

140

READS

35

8 AUTHORS, INCLUDING:



Eun Cheol Lee

Samsung SDI, Suwon, South Korea

16 PUBLICATIONS 1,037 CITATIONS

SEE PROFILE



Dongwook Kim

Kyonggi University

47 PUBLICATIONS 1,843 CITATIONS

SEE PROFILE



Tarakeshwar Pilarisetty

Arizona State University

99 PUBLICATIONS 4,649 CITATIONS

SEE PROFILE



Kwang-Sun Kim

Korea University of Technology and Education

554 PUBLICATIONS 30,466 CITATIONS

SEE PROFILE

Substituent Effects on the Edge-to-Face Aromatic Interactions

Eun Cheol Lee, Byung Hee Hong, Ju Young Lee, Jong Chan Kim, Dongwook Kim, Yukyung Kim, P. Tarakeshwar,[†] and Kwang S. Kim*

Contribution from the National Creative Research Initiative Center for Superfunctional Materials, Department of Chemistry, Division of Molecular and Life Sciences, Pohang University of Science and Technology, San 31, Hyojadong, Namgu, Pohang 790-784, Korea

Received July 22, 2003; E-mail: kim@postech.ac.kr

Abstract: The edge-to-face interactions for either axially or facially substituted benzenes are investigated by using ab initio calculations. The predicted maximum energy difference between substituted and unsubstituted systems is ~0.7 kcal/mol (~1.2 kcal/mol if substituents are on both axially and facially substituted positions). In the case of axially substituted aromatic systems, the electron density at the para position is an important stabilizing factor, and thus the stabilization/destabilization by substitution is highly correlated to the electrostatic energy. This results in its subsequent correlation with the polarization and charge transfer. Thus, the stabilization/destabilization by substitution is represented by the sum of electrostatic energy and induction energy. On the other hand, the facially substituted aromatic system depends on not only the electron-donating ability responsible for the electrostatic energy but also the dispersion interaction and exchange repulsion. Although the dispersion energy is the most dominating interaction in both axial and facial substitutions, it is almost canceled by the exchange repulsion in the axial substitution, whereas in the facial substitution, together with the exchange repulsion it augments the electrostatic energy. The systems with electron-accepting substituents (NO₂, CN, Br, Cl, F) favor the axial substituent conformation, while those with electron-donating substituents (NH₂, CH₃, OH) favor the facial substituent conformation. The interactions for the T-shape complex systems of an aromatic ring with other counterpart such as H₂, H₂O, HCl, and HF are also studied.

I. Introduction

Aromatic interactions are known to play a significant role in stabilizing protein tertiary structures, enzyme–substrate complexes, organic supramolecules, and organic nanomaterials.^{1–7}

Therefore, a clear understanding of these interactions in terms of nanorecognition⁸ is of importance for the design of novel supramolecular systems and nanomaterials. In particular, the discussion of the edge-to-face interactions in biomolecules by Burley and Petsko,¹ the spectral study of the van der Waals force in the benzene dimer by Schlag and co-workers,² the detailed systematic study of the aromatic interactions by Hunter and Saunders,³ by Cozzi, Siegel, and co-workers,⁴ and by Wilcox and co-workers⁵ have greatly impacted the studies of aromatic interactions for molecular assembly. However, the nature of aromatic interaction and the substituent effect is not clearly understood. Various studies on the benzene dimer have focused on the face-to-face (stacked), displaced face-to-face (displaced stacked), and edge-to-face (T-shaped) structures.^{9–13} Of these, the latter two are much more stable, with the last being

[†] Permanent Address: School of Computational Sciences, Korea Institute of Advanced Study, 207-43 Cheongnyangni 2-dong, Dongdaemun-gu, Seoul, 130-72, Korea.

- (1) (a) Burley, S. K.; Petsko, G. A. *Science* **1985**, 229, 23. (b) Burley, S. K.; Petsko, G. A. *Adv. Protein Chem.* **1988**, 39, 125. (c) Burley, S. K.; Petsko, G. A. *Trends Biotechnol.* **1989**, 7, 354.
- (2) (a) Bornsen, K. O.; Selzle, H. L.; Schlag, E. W. *J. Chem. Phys.* **1986**, 85, 1726. (b) Hobza, P.; Selzle, H. L.; Schlag, E. W. *J. Chem. Phys.* **1990**, 93, 5893.
- (3) (a) Hunter, C. A.; Sanders, J. K. M. *J. Am. Chem. Soc.* **1990**, 112, 5525. (b) Hunter, C. A. *Angew. Chem., Int. Ed. Engl.* **1993**, 32, 1584. (c) Hunter, C. A. *Chem. Soc. Rev.* **1994**, 23, 101. (d) Carver, F. J.; Hunter, C. A.; Livingstone, D. J.; McCabe, J. F.; Seward, E. M. *Chem.–Eur. J.* **2002**, 8, 2848.
- (4) Cozzi, F.; Cinquini, M.; Annunziata, R.; Dwyer, T.; Siegel, T. S. *J. Am. Chem. Soc.* **1992**, 114, 5729.
- (5) (a) Paliwal, S.; Geib, S.; Wilcox, C. S. *J. Am. Chem. Soc.* **1994**, 116, 4497. (b) Kim, E.; Paliwal, S.; Wilcox, C. S. *J. Am. Chem. Soc.* **1998**, 120, 11192.
- (6) (a) Hong, B. H.; Lee, J. Y.; Lee, C.-W.; Kim, K. C.; Bae, S. C.; Kim, K. S. *J. Am. Chem. Soc.* **2001**, 123, 10748. (b) Hong, B. H.; Bae, S. C.; Lee, C.-W.; Jeong, S.; Kim, K. S. *Science* **2001**, 294, 348. (c) Kim, K. S.; Suh, S. B.; Kim, J. C.; Hong, B. H.; Lee, E. C.; Yun, S.; Tarakeshwar, P.; Lee, J. Y.; Kim, Y.; Ihm, H.; Kim, H. G.; Lee, J. W.; Kim, J. K.; Lee, H. M.; Kim, D.; Cui, C.; Youn, S. J.; Chung, H. Y.; Choi, H. S.; Lee, C.-W.; Cho, S. J.; Jeong, S.; Cho, J.-H. *J. Am. Chem. Soc.* **2002**, 124, 14268. (d) Tarakeshwar, P.; Choi, H. S.; Kim, K. S. *Chem. Rev.* **2000**, 100, 4145.
- (7) (a) Schladetzky, K. D.; Haque, T. S.; Gellman, S. H. *J. Org. Chem.* **1995**, 60, 4108. (b) Gellman, S. H. *Chem. Rev.* **1997**, 97, 1231. (c) Kim, C.-Y.; Chabdra, P. P.; Jain, A.; Christanson, D. W. *J. Am. Chem. Soc.* **2001**, 123, 9620. (d) Lee, H.; Knobler, C. B.; Hawthorne, M. F. *Angew. Chem., Int. Ed.* **2001**, 40, 3058. (e) Meyer, E. A.; Castellano, R. K.; Diederich, F. *Angew. Chem., Int. Ed.* **2003**, 42, 1210.
- (8) (a) Tarakeshwar, P.; Kim, K. S. Nanorecognition. In *Encyclopedia of Nanoscience and Nanotechnology*; Nalwa, H. S., Ed.; American Scientific Publishers: Stevenson Ranch, CA, 2004; Vol. 7, pp 367–404. (b) Kim, K. S.; Tarakeshwar, P.; Lee, H. M. De novo theoretical design of functional nanomaterials and molecular devices. In *Dekker Encyclopedia of Nanoscience and Nanotechnology*; Schwarz, J. A., Contescu, C., Putyera, K., Eds.; Marcel Dekker: New York, 2004; Vol. 3, pp 2423–2433. (c) Tarakeshwar, P.; Kim, D.; Lee, H. M.; Suh, S. B.; Kim, K. S. Theoretical Approaches to the Design of Functional Nanomaterials. In *Computational Materials Science*; Leszczynski, J., Ed.; Theoretical and Computational Chemistry Series; Elsevier: Amsterdam, 2004; Vol. 15, pp 119–170.
- (9) (a) Ren, T.; Jin, Y.; Kim, K. S.; Kim, D. H. *J. Biomol. Struct. Dyn.* **1997**, 15, 401. (b) Hong, B. H.; Lee, J. Y.; Cho, S. B.; Yun, S.; Kim, K. S. *J. Org. Chem.* **1999**, 64, 5661. (c) Kim, K. S.; Tarakeshwar, P.; Lee, J. Y. *J. Am. Chem. Soc.* **2001**, 123, 3323.
- (10) (a) Jorgensen, W. L.; Severance, D. L. *J. Am. Chem. Soc.* **1990**, 112, 4768. (b) Heidrich, D. *Angew. Chem., Int. Ed.* **2002**, 41, 3208.

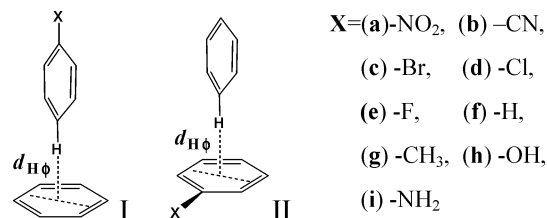


Figure 1. Model systems for aromatic edge-to-face interactions with various substituents. The CH atoms at the para position of the axial (vertical) ring are constrained to be along the axis passing through the center of the facial (horizontal) ring and to be perpendicular to the facial ring.

slightly more stabilized. Hence, the displaced stacked conformers are often found in organic crystals and nanomaterials, and the edge-to-face conformers are frequently found in biological systems. Wilcox and co-workers⁵ suggested that electrostatic energy (E_{elec}) alone cannot explain the T-shaped conformation and that the dispersion energy (E_{disp}) is important, using facial aromatic rings with electron-donating/accepting groups. Since the conformational changes between T-shape and stacked conformers could be utilized as precursors of nanomechanical devices¹⁴ such as molecular vessels for drug delivery and nano-surgery, the understanding of edge-to-face interaction between the edge H atom of an axial aromatic ring and the center of the facial aromatic ring is of importance.

It is generally known that the substituent effect on the aromatic ring is related to both the inductive effect caused by the electronegativity of substituent (electron-localization factor) and the resonance effect (electron-delocalization factor). These effects are highly correlated to Hammett's constants.¹⁵ In terms of the inductive effects, the NH_2 , OH, F, Cl, Br, CN, and NO_2 groups are electron acceptors, while CH_3 is an electron donor. However, in terms of resonance effects, the NH_2 , OH, F, Cl, Br, and CH_3 groups are electron donors, while CN and NO_2 are electron acceptors. NH_2 and OH have some of the electron-accepting inductive effects due to the electronegativity of N and O atoms, but their electron-donating resonance effects are dominating. Although the F, Cl, and Br groups have some of the electron-donating resonance effects, the electron-accepting inductive effects are dominating. Therefore, the F, Cl, Br, CN, and NO_2 groups have negative Hammett's constants as electron acceptors, while the NH_2 , OH, and CH_3 groups have positive Hammett's constants as electron donors.

In continuation of our investigations initiated several years ago,¹⁶ we compare edge-to-face interactions of variously substituted aromatic systems at reliable levels of ab initio calculations on model systems I and II with substituted axial

and facial benzenes, respectively (Figure 1). In addition, we have studied the edge-to-face interactions for the complex systems of a facial aromatic ring with an axial counterpart such as H_2 , H_2O , HCl , and HF . This study would be useful for the design of novel supramolecular systems and molecular devices and the understanding of T-shaped structures in biomolecular systems due to the edge-to-face interactions.

II. Calculation Methods

To investigate electron-accepting and -donating effects for edge-to-face complexes of a benzene molecule interacting with variously substituted aromatic rings, we performed ab initio calculations using Gaussian 98 and Molpro programs.¹⁷ The charges were obtained using natural bond orbital (NBO)¹⁸ analysis. The initial structures of types I and II were optimized (with the axial ring constrained to be perpendicular to the facial ring, as shown in Figure 1) at the level of Moller–Plesset second-order perturbation theory (MP2) using the 6-31+G* basis set. The MP2/6-311++G** interaction energies on the MP2/6-31+G* geometries were calculated for comparison. The interphenyl distances ($d_{\text{H}\phi}$) (between the axial H and facial center) for the MP2/6-31+G* structures I and II were optimized with the basis set superposition error (BSSE)-corrected MP2 calculations using the aug-cc-pVDZ basis set (to be shortened as aVDZ). We also carried out the coupled cluster calculations with singles and doubles excitations (CCSD) and those including perturbative triples excitations [CCSD-(T)] using aug-cc-pVDZ' (to be shortened as aVDZ') wherein the diffuse functions for H and the d diffuse functions for other atoms are deleted. For investigation of the interphenyl charge transfer, we used NBO at the MP2/aVDZ level. Since the size of basis sets is very important for the study of aromatic interactions, we carried out MP2 calculations using the aug-cc-pVTZ basis set (to be shortened as aVTZ) on the above MP2/aVDZ geometries. To consider the solvent effect, the relative interaction energy in the chloroform ($\epsilon = 4.9$) solvent ($\delta\Delta E_{\text{sol}}$) was obtained by using the isodensity surface polarized continuum model (IPCM) at the MP2/6-31+G* level. To understand the nature of the interaction energies, we evaluated the electrostatic energies, induction energies, dispersion energies, and exchange repulsion energies, with the symmetry adapted perturbation theory (SAPT)¹⁹ using the aVDZ' basis set. The molecular orbital (MO) analysis was done using the Pismo package.²⁰

III. Results

Table 1 lists the interaction energies (ΔE), interphenyl charge transfer (q_{CT}), and interphenyl distances ($d_{\text{H}\phi}$) along with the

- (11) (a) Hobza, P.; Šponer, J. *J. Am. Chem. Soc.* **2002**, *124*, 11802. (b) Hobza, P.; Selzle, H. L.; Schlag, E. W. *J. Phys. Chem.* **1996**, *100*, 18790. (c) Hobza, P.; Selzle, H. L.; Schlag, E. W. *J. Am. Chem. Soc.* **1994**, *116*, 3500. (d) Hobza, P.; Selzle, H. L.; Schlag, E. W. *Chem. Rev.* **1994**, *94*, 1767.
- (12) (a) Lindeman, S. V.; Kosynkin, D.; Kochi, J. K. *J. Am. Chem. Soc.* **1998**, *120*, 13268. (b) Brutschy, B. *Chem. Rev.* **2000**, *100*, 3891. (c) Tsuzuki, S.; Honda, K.; Uchimaru, T.; Mikami, M.; Tanabe, K. *J. Am. Chem. Soc.* **2002**, *124*, 104. (d) Wang, Y.; Hu, X. *J. Am. Chem. Soc.* **2002**, *124*, 8445. (e) Scheiner, S.; Kar, T.; Pattanayak, J. *J. Am. Chem. Soc.* **2002**, *124*, 13257.
- (13) (a) Sinnokrot, M. S.; Valeev, E. F.; Sherrill, C. D. *J. Am. Chem. Soc.* **2002**, *124*, 10887. (b) Sinnokrot, M. S.; Sherrill, C. D. *J. Phys. Chem. A* **2003**, *107*, 8377.
- (14) (a) Kim, H. G.; Lee, C.-W.; Yun, S.; Hong, B. H.; Kim, Y.-O.; Kim, D.; Ihm, H.; Lee, J. W.; Lee, E. C.; Tarakeshwar, P.; Park, S.-M.; Kim, K. S. *Org. Lett.* **2002**, *4*, 3971. (b) Manojkumar, T. K.; Choi, H. S.; Hong, B. H.; Tarakeshwar, P.; Kim, K. S. *J. Chem. Phys.* **2004**, *121*, 841.
- (15) (a) Hammett, L. P. *Chem. Rev.* **1935**, *17*, 125. (b) Hammett, L. P. *J. Am. Chem. Soc.* **2002**, *124*, 8445. (c) Pines, S. H. *Organic Chemistry*, McGraw-Hill: New York, 1987. (d) Solomons, T. W. G., Ed. *Organic Chemistry*; Wiley: New York, 1996.
- (16) (a) Lee, J. Y. B.S. Dissertation, Pohang University of Science and Technology, Pohang, Korea, 1992. (b) Lee, S. J. Ph.D. Dissertation, Pohang University of Science and Technology, Pohang, Korea, 1996. (c) Hong, B. H. M.S. Dissertation, Pohang University of Science and Technology, Pohang, Korea, 2000.
- (17) (a) Frisch, M. J.; Trucks, G. W.; Schlegel, H. B.; Scuseria, G. E.; Robb, M. A.; Cheeseman, J. R.; Zakrzewski, V. G.; Montgomery, J. A., Jr.; Stratmann, R. E.; Burant, J. C.; Dapprich, S.; Millam, J. M.; Daniels, A. D.; Kudin, K. N.; Strain, M. C.; Farkas, O.; Tomasi, J.; Barone, V.; Cossi, M.; Cammi, R.; Mennucci, B.; Pomelli, C.; Adamo, C.; Clifford, S.; Ochterski, J.; Petersson, G. A.; Ayala, P. Y.; Cui, Q.; Morokuma, K.; Malick, D. K.; Rabuck, A. D.; Raghavachari, K.; Foresman, J. B.; Cioslowski, J.; Ortiz, J. V.; Stefanov, B. B.; Liu, G.; Liashenko, A.; Piskorz, P.; Komaromi, I.; Gomperts, R.; Martin, R. L.; Fox, D. J.; Keith, T.; Al-Laham, M. A.; Peng, C. Y.; Nanayakkara, A.; Gonzalez, C.; Challacombe, M.; Gill, P. M. W.; Johnson, B. G.; Chen, W.; Wong, M. W.; Andres, J. L.; Head-Gordon, M.; Replogle, E. S.; Pople, J. A. *Gaussian 98*, revision A.11; Gaussian, Inc.: Pittsburgh, PA, 1998. (b) Amos, R. D.; Bernhardsson, A.; Berning, A.; Celani, P.; Cooper, D. L. et al. *MOLPRO*, a package of ab initio programs designed by Werner, H.-J.; Knowles, P. J., version 2002.6.
- (18) Reed, A. E.; Curtiss, L. A.; Weinhold, F. *Chem. Rev.* **1988**, *88*, 899.
- (19) (a) Jeziorski, B.; Moszynski, R.; Szalewicz, K. *Chem. Rev.* **1994**, *94*, 1887. (b) Jeziorski, B.; Szalewicz, K. *J. Chem. Phys.* **1995**, *95*, 6576. (c) Moszynski, R.; Korona, T.; Wormer, P. E. S.; van der Avoird, A. *J. Phys. Chem. A* **1997**, *101*, 4690. (d) Szalewicz, K.; Jeziorski, B. In *Molecular Interactions: From van der Waals to Strongly Bound Complexes*; Scheiner, S., Ed.; Wiley: New York, 1997; p 3.
- (20) Lee, S. J.; Chung, H. Y.; Kim, K. S. *Bull. Korean Chem. Soc.* **2004**, *25*, 1061.

Table 1. Relative Interaction Energies ($\Delta\Delta E$) and Interphenyl Charge Transfer (δq_{CT}) for the Edge-to-Face Aromatic Interactions (Types I and II) and the Hammett's Substituent Constants (σ_p) for p -C₆H₅X^a

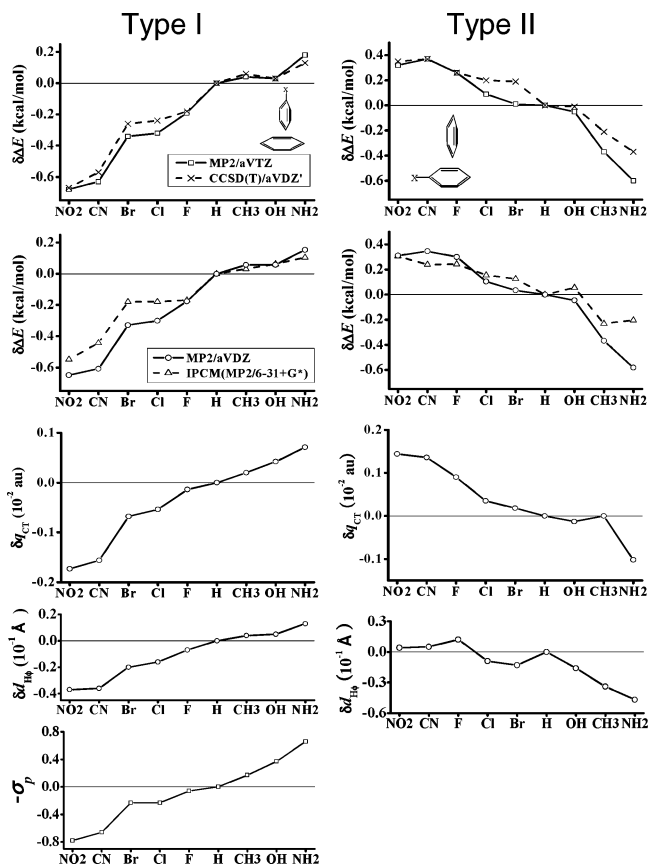
type I: X	← strong electron-accepting				strong electron-donating →				
	NO ₂	CN	Br	Cl	F	CH ₃	OH	NH ₂	(H)
δE : MP2/6-31+G*	-0.68	-0.59	-0.31	-0.26	-0.22	0.05	0.04	0.15	(ΔE : -1.60)
MP2/6-311++G**	-0.63	-0.57	-0.27	-0.23	-0.18	0.05	0.06	0.17	(ΔE : -2.31)
MP2/aVDZ	-0.65	-0.61	-0.33	-0.30	-0.18	0.06	0.06	0.15	(ΔE : -3.20)
MP2/aVTZ	-0.68	-0.63	-0.34	-0.30	-0.17	0.06	0.05	0.18	(ΔE : -3.44)
CCSD(T)/aVDZ'	-0.67	-0.57	-0.26	-0.24	-0.18	0.06	0.03	0.13	(ΔE : -1.56)
$\delta\Delta E_{soln}$: MP2/6-31+G*	-0.55	-0.44	-0.18	-0.18	-0.17	0.03	0.06	0.10	(ΔE_{soln} : -1.47)
$\delta_{H\phi}$: MP2/aVDZ	-0.037	-0.036	-0.020	-0.016	-0.007	0.004	0.005	0.013	($d_{H\phi}$: 2.466)
δq_{CT} : MP2/aVDZ	-0.17	-0.16	-0.07	-0.05	-0.01	0.02	0.04	0.07	(q_{CT} : -1.33)
$\delta q_{H+C/4}(p)$: MP2/aVDZ	0.90	0.90	0.40	0.35	0.16	-0.09	-0.23	-0.49	($q_{H+C/4}(p)$: 16.7)
σ_p	0.78	0.66	0.23	0.23	0.06	-0.17	-0.37	-0.66	0

type II: X	CN	NO ₂	F	Cl	Br	OH	CH ₃	NH ₂	(H)
$\delta\Delta E$: MP2/6-31+G*	0.38	0.38	0.31	0.26	0.22	0.04	-0.24	-0.36	(ΔE : -1.60)
MP2/6-311++G**	0.34	0.32	0.27	0.18	0.11	-0.02	-0.32	-0.39	(ΔE : -2.31)
MP2/aVDZ	0.34	0.31	0.30	0.10	0.03	-0.05	-0.37	-0.58	(ΔE : -3.20)
MP2/aVTZ	0.39	0.34	0.28	0.09	0.01	-0.05	-0.38	-0.60	(ΔE : -3.44)
CCSD(T)/aVDZ'	0.37	0.35	0.26	0.20	0.19	-0.01	-0.21	-0.37	(ΔE : -1.56)
$\delta\Delta E_{soln}$: MP2/6-31+G*	0.24	0.30	0.24	0.15	0.12	0.05	-0.23	-0.21	(ΔE_{soln} : -1.47)
$\delta_{H\phi}$: MP2/aVDZ	0.005	0.004	0.012	-0.009	-0.013	-0.016	-0.034	-0.047	($d_{H\phi}$: 2.466)
δq_{CT} : MP2/aVDZ	0.14	0.14	0.09	0.03	0.01	-0.02	-0.01	-0.10	(q_{CT} : -1.33)

^a All these values were obtained with BSSE correction. The relative interaction energies in the chloroform solvent (dielectric constant: $\epsilon = 4.9$) ($\delta\Delta E_{soln}$) were obtained using IPCM. The interphenyl distances $d_{H\phi}$ of MP2/6-31+G* optimized geometries were re-optimized with the BSSE-corrected MP2/aug-cc-pVDZ calculations. Energies are in kilocalories per mole, charges in 10^{-2} au, distances in angstroms. The values in the table (except for those in parentheses for the cases of X = H for which the absolute values are given) are relative values with respect to the T-shaped benzene dimer. σ_p is Hammett's substituent constant for the para positions, defined as the acidities of p -substituted benzoic acid at 25 °C. The charge of $\Delta q_{H+C/4}$ ($= \Delta q_H + \Delta q_{C/4}$) at the para position is strongly correlated with σ_p and $\delta\Delta E$, because the induction energy is proportional to αE^2 , where α is the polarizability of the facial benzene and E is the electric field ($E = q/d^2$) where the facial aromatic ring center is at the distances ($d_{H\phi} = 2.47$ Å and $d_{C\phi} = 3.55$ Å) from the atomic charge q of the edge atoms (p -H and p -C) in the axial aromatic rings. Then, the induction energy is approximately proportional to $\alpha(q_H/2.47^2 + q_C/3.55^2) \approx \alpha(q_H + q_C/4)/(2.47)^2$. It should be noted that both all the relative energies at the different levels of theory are consistent, while their absolute magnitudes vary depending on the levels of theory.

plot of Hammett constants (σ_p) versus substituent groups. $\delta\Delta E$, δq_{CT} , and $\delta d_{H\phi}$ are the relative values for the substituted systems with respect to the unsubstituted benzene dimer. The relative values are depicted in Figure 2. The absolute binding energy of the benzene dimer depends seriously on the levels of theory and basis sets. The binding energy ($-\Delta E$) of MP2/6-31+G*, MP2/6-311++G**, MP2/aVDZ, MP2/aVTZ, MP2/aVQZ, CCSD/aVDZ', and CCSD(T)/aVDZ' are 1.60, 2.31, 3.20, 3.44, 3.53, 1.10, and 1.56 kcal/mol, respectively. Therefore, the MP2/aVTZ value would be near the complete basis limit (CBS), which is estimated to be ~ 3.6 kcal/mol, while the CCSD(T)/aVDZ' value is far from the CBS value since the CCSD(T) calculations would require much larger basis sets to describe the CBS value than the MP2 calculations. If we assume that the CCSD(T)/aVDZ' binding energy is 1.28 kcal/mol smaller than the MP2/aVDZ' value, the CCSD(T) CBS binding energy could be estimated to be only ~ 2.3 kcal/mol.

Although the absolute binding energy depends seriously on the levels of theory and basis sets, it is interesting to note that the relative binding energies of the substituted aromatic systems do not significantly change, partially due to the cancellation errors. For example, the relative energies are almost the same within 0.02 kcal/mol for both CCSD(T)/aVDZ' and CCSD/aVDZ' (thus, the latter values have not been reported in Table 1), while the absolute binding energies of the former are consistently ~ 0.46 kcal/mol larger than those of the latter. Similarly, the MP2 binding energies are quite different depending on the basis set used, but the relative energy differences are almost same. The relative binding energies at the CCSD(T) level are similar to those at the MP2 level regardless of the basis set employed. In this regard, it is clear that the relative energies can be predicted in a reliable way, and therefore the

**Figure 2.** Relative values of interaction energies ($\delta\Delta E/\delta\Delta E_{sol}$ for the gas/solution phase; in kilocalories per mole), charge transfers (δq_{CT} in au), and interphenyl distances ($\delta d_{H\phi}$ in angstroms)) for types I and II, and the plot for σ_p vs type I substituent.

present discussion is equally valid at all levels of calculation reported here (partly except for the relative binding energies at the MP2/6-31+G* level, which uses only a small basis set). Only some careful consideration would be required (i.e., the interphenyl distances need to be properly optimized) when the different levels of calculation would give significant geometry changes toward the hard wall region in the interphenyl distance. In this regard, though all the results are consistent, there can be subtle errors up to ~0.1 kcal/mol (or at most ~0.2 kcal/mol in the worst situation). Considering that our results are based on geometries at the BSSE-corrected MP2/aVDZ level, we discuss our results in terms of MP2/aVDZ values [and MP2/aVTZ//MP2/aVDZ values in brackets], unless otherwise specified.

The interaction energy increase/decrease due to the mono-substitution of the benzene dimer is no more than 0.65/0.34 [0.68/0.39] kcal/mol in the gas phase. This value becomes much smaller (0.55/0.24 kcal/mol) in the chloroform solvent (dielectric constant $\epsilon = 4.9$). This small energy difference agrees with Wilcox's⁵ and our^{9a} previous experiments. Given that the edge-to-face interaction energy at the CCSD(T)/CBS level would be ~1.5 kcal/mol, these small energy changes would not be simply neglected. Though the energy changes by the substitution are small, the sum of a large number of these interaction terms could be significant in multisubstituted aromatic systems, in particular, in the cases when strong interactions are absent.

On the basis of the predicted interaction energies, we find that for type I, the electron-accepting strength of the axial aromatic ring is in the order $\text{NO}_2 > \text{CN} > \text{Br} > \text{Cl} > \text{F} > \text{H} > \text{CH}_3 > \text{OH} > \text{NH}_2$ in both the gas phase and the chloroform solution. For type II, the electron-donating strength of the facial aromatic ring is in the order $\text{CN} < \text{NO}_2 < \text{F} < \text{Cl} < \text{Br} < \text{H} < \text{OH} < \text{CH}_3 < \text{NH}_2$ in the gas phase and in the order $\text{NO}_2 < \text{CN} < \text{F} < \text{Cl} < \text{Br} < \text{OH} < \text{H} < \text{NH}_2 \approx \text{CH}_3$ in the chloroform solution. Therefore, the order in binding strength of type I for NO_2 and CN in the gas phase, that for Br , Cl , and F in both gas and solution phases, that for CH_3 and OH in the gas phase, and that for CH_3 and NH_2 in the chloroform solution are changed in type II. It should be noted that though the systems with electron-accepting substituents (NO_2 , CN , Br , Cl , F) favor type I, those with electron-donating substituents (NH_2 , CH_3 , OH) favor type II; then the substitution can strengthen the binding, compared to the unsubstituted benzene dimer.

For type I, the binding strength (related to $-\Delta E$) increases as the substituent changes from strong electron donor to strong electron acceptor. The trend for ΔE is consistent with those for q_{CT} and $d_{\text{H}\phi}$. Cozzi, Siegel, and co-workers⁴ have shown a good correlation between the free energy and the Hammett constant. Indeed, we also find that ΔE and consequently q_{CT} and $d_{\text{H}\phi}$ are correlated with the Hammett constant at para position (σ_{p}), while they are not correlated with the reaction constant. In particular, the edge-to-face interaction energy change by substitution ($\delta\Delta E$) for type I is strongly correlated with δq_{CT} and $\delta d_{\text{H}\phi}$. The interaction for type I can thus be correlated with the charge transfer effect or polarizability-driven inductive effect. Among the halide substituents, the Br substituent has larger energy gain (0.33 kcal/mol) due to the large polarizability of Br , while the substituted system by a highly electronegative F atom shows small binding energy gain (0.18 kcal/mol). Thus, for type I, the polarizability-driven inductive effect would be important. For type I, a strong electron-accepting/donating group of the NO_2/NH_2 substituent

increases/decreases the binding strength by 0.65/0.15 [0.68/0.18] kcal/mol compared to the unsubstituted case. The solvent effect for type I does not change the order in binding strength in the gas phase, but slightly decreases the absolute binding energy and the relative binding energy differences.

For type II, the increased/decreased π -electron density by the electron-donating/accepting substituent NH_2/CN increases/decreases the binding strength by 0.58/0.34 [0.60/0.39] kcal/mol. The solvent effect changes the order in binding strength between NO_2 and CN and the order between CH_3 and NH_2 . The largest/smallest binding energy in solution is 1.70/1.17 kcal/mol (for CH_3/NO_2), while that in the gas phase is 3.79/2.86 kcal/mol (for NH_2/CN). The maximum binding energy gain/loss by substituent in the benzene dimer is only 0.23/0.30 kcal/mol in the solvent, in contrast to significant gain/loss in the gas phase 0.38/0.36 kcal/mol at MP2/6-31+G* (0.58/0.34 kcal/mol at MP2/aVDZ). Although in solution CN/CH_3 is a more effective electron-acceptor/donor than NO_2/NH_2 , the overall trend in solvent is similar to that in the gas phase. In addition, considering the halide groups that are electron-acceptors, the F -substituent system is more stabilized than the Cl/Br substituent systems, so this trend is opposite to that in type I. Similarly, the OH group is less effective than the CH_3 group. In addition to the charge transfer from the facial to axial rings, the $\text{CH}-\pi$ interaction in type II depends on the electron density around the center of a substituted facial aromatic ring which is very sensitive to the exchange repulsion and dispersion energy.

For the complexes involving both types I and II, the interaction energies are found to be nearly additive. The complex with the facial aminobenzene and the axial nitrobenzene gives the interaction energy gain by 1.18 kcal/mol over the dimer. This value is close to the sum (1.23 kcal/mol) of the interaction energy gain (0.65 kcal/mol) for the axial nitrobenzene interacting with the benzene and that (0.58 kcal/mol) for the facial aminobenzene interacting with the benzene. The complex with the facial cyanobenzene and the axial nitrobenzene gives the interaction energy gain by 1.16 kcal/mol over the dimer, close to the sum of the two separate contributions (0.61 + 0.58 = 1.19 kcal/mol). Thus, the edge-to-face interactions can be enhanced as much as 1.2 kcal/mol by both axial and facial substitutions.

Using SAPT at the MP2/aVDZ' level, we carried out the decomposition of the interaction energies of types I and II:

$$E_{\text{tot}} = E_{\text{es}} + E_{\text{exch}} + E_{\text{ind}} + E_{\text{disp}} + \delta_{\text{int,resp}}^{\text{HF}}$$

$$= E_{\text{es}} + E_{\text{exch}}^* + E_{\text{ind}}^* + E_{\text{disp}}^* + \delta_{\text{int,resp}}^{\text{HF}}$$

where

$$E_{\text{es}} = E_{\text{es}}^{(10)} + E_{\text{es,resp}}^{(12)}$$

$$E_{\text{ind}} = E_{\text{ind}}^{(20)}$$

$$E_{\text{disp}} = E_{\text{disp}}^{(20)}$$

$$E_{\text{exch}} = E_{\text{exch}}^{(10)} + E_{\text{exch}}^{(11)} + E_{\text{exch}}^{(12)} + E_{\text{exch,ind,resp}}^{(20)} + E_{\text{exch,disp}}^{(20)}$$

$$E_{\text{ind}}^* = E_{\text{ind}}^{(20)} + E_{\text{exch,ind,resp}}^{(20)}$$

$$E_{\text{disp}}^* = E_{\text{disp}}^{(20)} + E_{\text{exch,disp}}^{(20)}$$

Table 2. Substituent Effect (Relative Energy with Respect to the Basis Set at the MP2/aVDZ' Level) of the Interaction Energies and Energy Components (Kilocalories per Mole) for the Edge-to-Face Aromatic Interactions (Types I and II) by SAPT Decomposition.

type I: X	NO ₂	CN	Cl	OH	NH ₂	(H)
δE_{tot}	-0.77	-0.66	-0.28	0.05	0.19	(E_{tot} : -2.49)
δE_{es}	-0.59	-0.55	-0.25	0.05	0.20	(E_{es} : -2.04)
δE_{ind}	-0.24	-0.20	-0.08	0.01	0.03	(E_{ind} : -1.00)
δE_{ind}^*	-0.17	-0.13	-0.05	0.01	0.02	(E_{ind}^* : -0.23)
$\delta \delta_{\text{int,resp}}^{\text{HF}}$	-0.10	-0.09	-0.04	0.01	0.03	($\delta_{\text{int,resp}}^{\text{HF}}$: -0.35)
δE_{disp}	-0.17	-0.19	-0.09	0.01	0.02	(E_{disp} : -4.56)
δE_{disp}^*	-0.17	-0.18	-0.09	0.01	0.02	(E_{disp}^* : -4.10)
δE_{exch}	0.33	0.37	0.18	-0.04	-0.09	(E_{exch} : 5.47)
δE_{exch}^*	0.26	0.30	0.14	-0.03	-0.08	(E_{exch}^* : 4.24)
$\delta E_{\text{es+ind}}^*$	-0.76	-0.68	-0.29	0.06	0.22	($E_{\text{es+ind}}^*$: -2.27)
$\delta E_{\text{disp}^*+\text{exch}^*+\delta\text{HF}}$	-0.01	0.02	0.01	-0.01	-0.03	($E_{\text{disp}^*+\text{exch}^*+\delta\text{HF}}$: -0.21)
E_{corr}	-0.16	-0.03	0.01	-0.02	-0.05	(E_{corr} : -3.75)
type II: X	NO ₂	CN	Cl	OH	NH ₂	(H)
δE_{tot}	0.33	0.34	0.13	-0.03	-0.45	(E_{tot} : -2.49)
δE_{es}	0.50	0.52	0.26	-0.04	-0.54	(E_{es} : -2.04)
δE_{ind}	0.04	0.06	-0.01	-0.08	-0.25	(E_{ind} : -1.00)
δE_{ind}^*	0.08	0.08	0.04	0.00	-0.05	(E_{ind}^* : -0.23)
$\delta \delta_{\text{int,resp}}^{\text{HF}}$	0.08	0.07	0.03	-0.02	-0.08	($\delta_{\text{int,resp}}^{\text{HF}}$: -0.35)
δE_{disp}	-0.12	-0.13	-0.22	-0.20	-0.58	(E_{disp} : -4.56)
δE_{disp}^*	-0.16	-0.16	-0.22	-0.18	-0.50	(E_{disp}^* : -4.10)
δE_{exch}	-0.18	-0.19	0.12	0.26	0.98	(E_{exch} : 5.47)
δE_{exch}^*	-0.18	-0.19	0.07	0.16	0.70	(E_{exch}^* : 4.24)
$\delta E_{\text{disp}^*+\text{exch}^*}$	-0.34	-0.35	-0.15	-0.02	0.20	($E_{\text{disp}^*+\text{exch}^*}$: 0.14)
$\delta E_{\text{es+disp}^*+\text{exch}^*}$	0.16	0.17	0.11	-0.06	-0.34	($E_{\text{es+disp}^*+\text{exch}^*}$: -1.90)
E_{corr}	-0.44	-0.35	-0.32	-0.23	-0.45	(E_{corr} : -3.75)

and

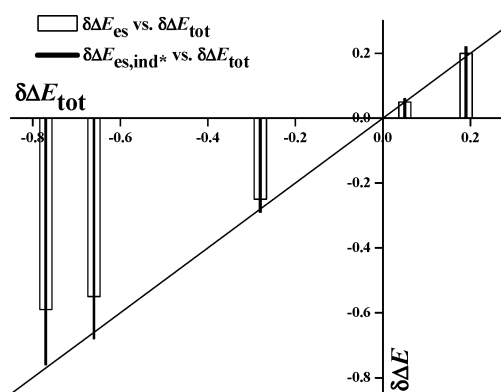
$$E_{\text{exch}}^* = E_{\text{exch}}^{(10)} + E_{\text{exch}}^{(11)} + E_{\text{exch}}^{(12)}$$

Here the first number 1 or 2 in parentheses in superscript indicates the first- or second-order perturbation term; the second number 0/1/2 in parentheses in superscript indicates the zeroth/first/second-order correction; the notations in subscripts mean the following; tot: total energy, ind: induction, disp: dispersion, exch: exchange, and $\delta_{\text{int,resp}}^{\text{HF}}$: all induction and exchange-induction terms of order higher than the second. The “resp” indicates that a given component has been computed including the coupled Hartree–Fock response for the perturbed system, and “ E_{corr} ” is the sum of the correlation components. The superscript “*” indicates the effective energy component.

The substituent effects of the interaction energies and energy components for types I and II are listed in Table 2. In the benzene dimer, we find that the total interaction energy (E_{tot}) is -2.49 kcal/mol, and the electrostatic energy (E_{es}), induction energy (E_{ind}), dispersion energy (E_{disp}), and exchange repulsion (E_{exch}) are -2.04, -1.00, -4.56, and 5.47 kcal/mol, respectively, and E_{ind}^* , E_{disp}^* , and E_{exch}^* are -0.23, -4.10, and -4.24 kcal/mol, respectively. Therefore, the dispersion is the dominating interaction component for any substituents in both types, since the substitution effect is not more than ~0.7 kcal/mol.

While the total interaction energies and their energy components widely vary depending on the levels of calculation, the relative energies little depend on them. Therefore, the relative energies (δE_{tot} , δE_{es} , δE_{exch} , δE_{ind} , δE_{disp}) of the substituted systems with respect to the benzene dimer are considered to be reliable. For both types, it is interesting to note that though the main energy component of E_{tot} is E_{disp} , the main energy component of δE_{tot} is δE_{es} . For type I, δE_{tot} is well described simply by δE_{es} among the four components (δE_{es} , δE_{exch} , δE_{ind} , δE_{disp}). Since the electrostatic energy plays a key role in type

I, the electrostatic energy-driven polarization (induction) is well correlated with E_{tot} . This well explains Hunter and Saunders' notion^{3a} that the induction is the subsequent effect due to the major electrostatic interaction component. We particularly note that $\delta E_{\text{es+ind}}^*$ ($= \delta E_{\text{es}} + \delta E_{\text{ind}}^*$) is almost the same as δE_{tot} , since the three terms of δE_{disp}^* , δE_{exch}^* , and δE_{HF} ($\delta E_{\text{disp}^*+\text{exch}^*+\delta\text{HF}} = \delta E_{\text{disp}}^* + \delta E_{\text{exch}}^* + \delta E_{\text{HF}}$) almost cancel out. Thus, the total energy change by the substituent effect in type I is represented by the sum of δE_{es} and δE_{ind}^* . One can easily note a good correlation between δE_{tot} and δE_{es} as well as an excellent agreement between δE_{tot} and $\delta E_{\text{es+ind}}^*$ (Figure 3).

**Figure 3.** $\delta \Delta E_{\text{es}}$ and $\delta \Delta E_{\text{es,ind}}^*$ vs $\delta \Delta E_{\text{tot}}$ linear fits for type I. Energies are in kilocalories per mole.

For type II, δE_{tot} is the most correlated with δE_{es} among the four components. In addition, $\delta E_{\text{es+disp}^*+\text{exch}^*}$ ($= \delta E_{\text{es}} + \delta E_{\text{disp}}^* + \delta E_{\text{exch}}^*$) is also correlated with δE_{tot} (Figure 4). Thus, the substituent effect in type II is complicated. The decrease/increase of the electron density of the facial rings by large/small charge transfer due to the electron-donor/acceptor should significantly decrease/increase δE_{ind} , but this change is less significant than

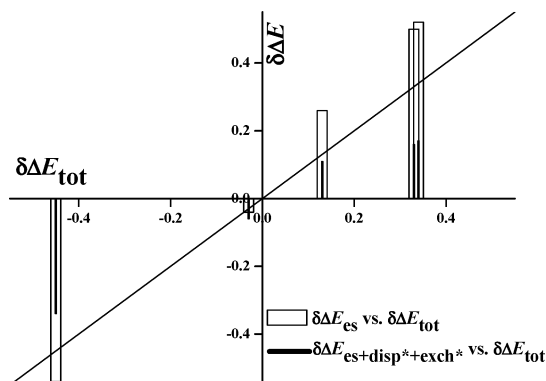


Figure 4. $\delta\Delta E_{\text{es}}$ and $\delta\Delta E_{\text{es+disp}^*+\text{exch}^*}$ vs $\delta\Delta E_{\text{tot}}$ linear fits for type II. Energies are in kilocalories per mole.

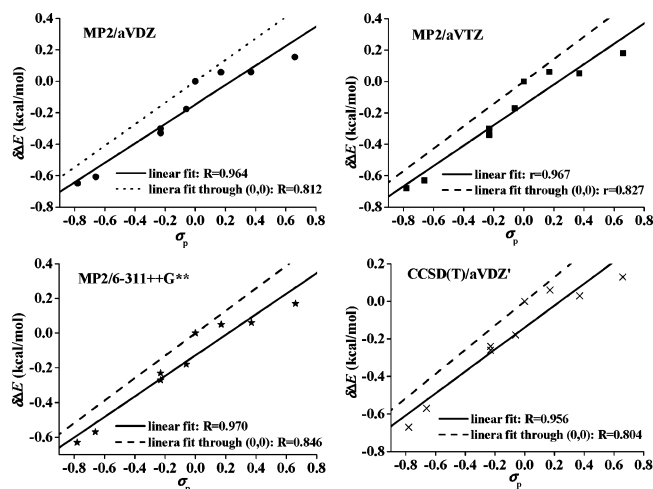


Figure 5. $\delta\Delta E$ vs σ_p linear fits for type I at various levels of calculation.

the changes of δE_{disp}^* and δE_{exch}^* . Upon substitution, δE_{disp}^* values are all greater in magnitude than that of the benzene dimer, probably because the total electron population of the facial benzene ring increases (since the H atom depletes the electron density of the facial aromatic ring as a strong electron acceptor, in comparison with non-hydrogen atoms). While the electron-donor/acceptor with increased/decreased charge transfer shows increased/decreased binding energy, the sum of δE_{ind} , δE_{exch} , and δE_{disp} reasonably differentiates various edge-to-face interactions for type II.

In contrast to the Hammett constant, which is highly correlated to the edge-to-face interaction for type I, there is no useful parameter to describe such interaction for type II. Thus, a new Hammett-like constant would be desirable. For type II, it would be more realistic to use $\delta\Delta E$ as a new parameter to describe the edge-to-face interaction. There is a good correlation between σ_p and $-\delta\Delta E$ for type I (r factor = 0.964 [0.967] for $\delta\Delta E = a\sigma_p + b$, a, b : constants; or r factor = 0.812 [0.827] for $\delta\Delta E = a\sigma_p$ when the case of the benzene dimer is fixed at the origin (0,0)) as shown in Figure 5. The case when X is H, due to the extremely small atomic size of H and the kinetic effect due to rapid exchange, is somewhat different from the case when X is a non-hydrogen atom. Thus, the constraint to fix the case of benzene dimer at the origin ($\delta\Delta E = k\sigma_p$) gives much less correlation. Nevertheless, the correlation is still effective. In this regard, it would be possible to define a comparable new parameter σ_p' with the value of $-\delta\Delta E$ for type I, where the positive/negative sign indicates an electron acceptor/

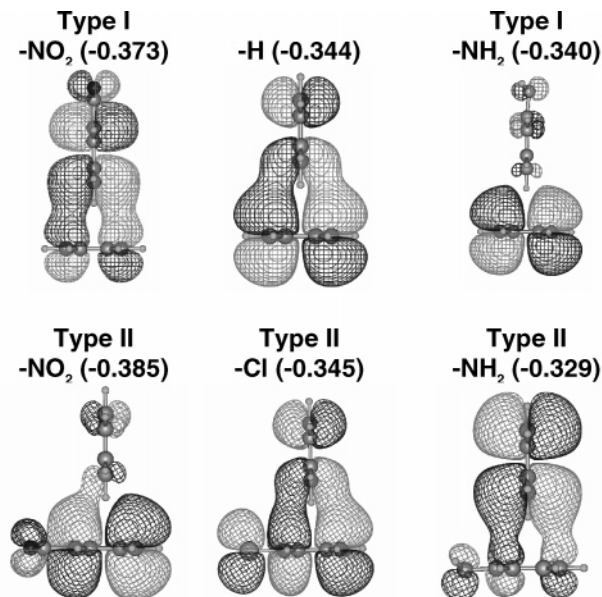


Figure 6. Occupied molecular orbitals of types I (top) and II (bottom) involved with the charge transfer. Orbital energies in parentheses are given in au. In contrast to the benzene dimer, which shows a moderate charge transfer ($q_{\text{CT}} = -0.0133$ au; $\delta q_{\text{CT}} = 0$ as a reference system), in the cases of type I the strong electron-accepting NO_2 group in the axial aromatic ring shows increased electron transfer toward the axial aromatic ring ($\delta q_{\text{CT}} = -0.0017$ au), whereas the strong electron-donating NH_2 group shows decreased charge transfer ($\delta q_{\text{CT}} = 0.0007$ au). In the cases of type II, the strong electron-accepting NO_2 groups in the facial aromatic rings show decreased charge transfers ($\delta q_{\text{CT}} = 0.00142$ au), while the strong electron-donating NH_2 group shows increased charge transfer ($\delta q_{\text{CT}} = -0.00103$ au).

electron donor. Similarly, it would be possible to define a new Hammett-like constant σ_c' with the value of $\delta\Delta E$ for type II (so that the positive/negative sign denotes an electron acceptor/electron donor). For example, the σ_c' for the facial substituent interaction would be defined on the basis of the relative binding energies predicted at various levels of theory (e.g., CN: 0.35, NO_2 : 0.35, F: 0.25, Cl: 0.2, Br: 0.05, OH: -0.05, CH_3 : -0.35, NH_2 : -0.5).

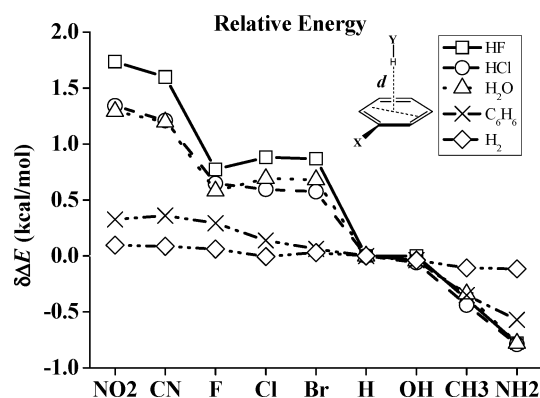
In the case of an axially substituted aromatic system, the Hammett's substituent constant and the electron density at the para position are important stabilizing factors, while the facially substituted aromatic system depends on not only the electron-donating ability but also the exchange repulsion and dispersion interaction. Therefore, Hammett-like constants σ_c' describe the edge-to-face interactions at the center of substituted aromatic rings, which would be useful for the study of protein structures and the design of molecular assembly-based devices.

Figure 6 shows interesting polarization effects on the occupied molecular orbitals of strong electron donor (NH_2) and strong electron acceptor (NO_2) substituted aromatic rings relative to the benzene ring for types I and II. The benzene gives only minor polarization from the facial ring to the axial ring. For type I, the strong electron-accepting group NO_2 withdraws electron (which results in strong stabilization), whereas the electron-donating group NH_2 forbids the electron withdrawing (which results in destabilization). Therefore, the polarization due to the electron donating/accepting power affects the edge-to-face interaction energy. This effect is very important in type I. In type II, the electrostatic interaction also plays an important role, and subsequently, the polarization is correlated with the

Table 3. Relative Energies of the T-Shaped Conformers of the X-Substituted Aromatic Ring Interacting with the Counter Molecules HY^a

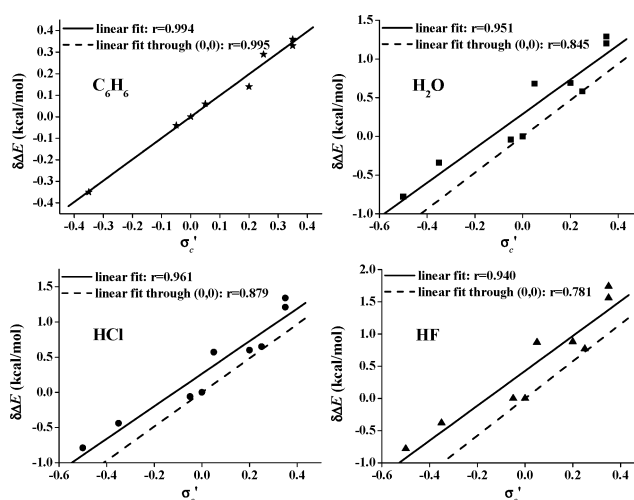
HYX	$(\delta\Delta E_{\text{e}}, \text{kcal/mol}) = \Delta E_{\text{e}}(\text{X}) - \Delta E_{\text{e}}(\text{H})$									(ΔE_{e})
	NO ₂	CN	F	Cl	Br	OH	CH ₃	NH ₂	H	
HF	1.74	1.56	0.77	0.88	0.87	0.00	-0.38	-0.78	-3.87	
HCl	1.34	1.21	0.65	0.60	0.57	-0.06	-0.44	-0.79	-4.19	
H ₂ O	1.29	1.20	0.58	0.69	0.68	-0.04	-0.34	-0.78	-2.85	
C ₆ H ₆	0.33	0.36	0.29	0.14	0.06	-0.04	-0.35	-0.57	-3.15	
H ₂	0.10	0.09	0.06	-0.00	0.03	-0.04	-0.11	-0.12	-0.92	

^a Calculations were carried out at the MP2/aug-cc-pVDZ/MP2/6-31+G* level.

**Figure 7.** Relative interaction energies ($\delta\Delta E$ in kilocalories per mole) for the T-shape conformers of the substituted aromatic ring with H₂, benzene, H₂O, HCl, and HF.

electrostatic energy. The facial NO₂-substituted aromatic ring forbids the electron transfer-driven polarization to the axial ring (which results in destabilization), whereas the facial NH₂-substituted aromatic ring allows strong polarization to the vertical ring (which results in strong stabilization). It is also interesting to note that the polarization for the facial Cl/Br/F-substituted aromatic ring in type II is slightly weaker than or similar to that for the benzene dimer system. However, other effects (dispersion and exchange in addition to the electrostatic energy) are also important in type II, as discussed earlier.

It is interesting to compare the edge-to-face interactions for the T-shaped aromatic–aromatic complexes with those for the T-shaped structure with an aromatic ring and a counterpart such as H₂, H₂O, HCl, and HF.²¹ In this case, H₂ would involve mainly dispersion and induction energies; the benzene involves dispersion, quadrupole-driven polarization, and quadrupole–quadrupole interaction energies; H₂O, HCl, and HF would involve dispersion, dipole-driven polarization, and dipole–quadrupole interaction energies. The dipole moments of H₂O, HCl, and HF along the axial direction are 1.13, 1.18, and 1.84 D, respectively. While the H₂ does not give significant interaction energy gain/loss depending on the substituted benzene, the quadrupole-driven electrostatic effect in the benzene shows marginal energy differences, and the dipole-driven electrostatic effects in H₂O, HCl, and HF show large energy differences depending upon substitution (Table 3 and Figure 7). In the case of H₂O, the difference in the edge-to-face interaction energy between the NO₂ and NH₂ cases is 2.1 kcal/mol. In the case of HF aromatic systems, this difference is further enhanced as much as 2.6 kcal/mol. The energy difference between the NO₂/NH₂-

**Figure 8.** $\delta\Delta E$ vs σ_c' linear fits for the T-shape conformers of the facially substituted aromatic ring interacting with C₆H₆, H₂O, HCl, and HF. The values of σ_c' are chosen as CN: 0.35, NO₂: 0.35, F: 0.25, Cl: 0.2, Br: 0.05, OH: -0.05, CH₃: -0.35, NH₂: -0.5.

substituted benzene–water system and the benzene–water system is 1.3/−0.8 kcal/mol; thus, these large energy differences would be useful for the design of novel supramolecular systems and novel molecular devices. Even though the difference in the aromatic–aromatic systems is not large, the sum of a large number of interactions in the absence of H-bonding-type interactions would be of importance to play a key role, which can be evidenced from the fact that the aromatic–aromatic π -stacking which has the interaction energy comparable to the edge-to-face interaction plays a key role in crystal packing.

Figure 8 shows the $\delta\Delta E$ versus σ_c' linear fit for the T-shape conformers of the substituted aromatic ring interacting with C₆H₆, H₂O, HCl, and HF. It shows reasonable correlations between $\delta\Delta E$ and σ_c' , which shows the validity of the defined Hammett-like constant σ_c' for the facial aromatic interactions.

IV. Conclusion

We compared the edge-to-face interactions for variously substituted aromatic systems, using ab initio calculations on model systems I and II with substituted axial and facial benzenes, respectively. In particular, for both model systems, we have focused our attention on elucidating the origin of energy differences between nine different substituents including nitro- and aminobenzenes as the extreme cases of the aromatic interactions. Though the total interaction energy widely varies depending on the levels of theory and basis sets employed, the interaction energy change by substitution varies little. Thus, our results are considered to be reliable. We note a clear difference in aromatic interactions between facial and axial substitutions. In both types, the dispersion energy is the dominating interaction energy component. Nevertheless, its effect is negligible in type I, while it plays only a subsidiary role in type II. In the case of axially substituted aromatic systems, the electron density at the para position is an important stabilizing factor, and thus the stabilization/destabilization by substitution of an aromatic ring is governed mostly by the electrostatic energy. This results in its subsequent correlation with the polarization and charge transfer. In a while, the dispersion energy is canceled out by the exchange repulsion. Thus, the stabilization/destabilization by substitution is represented simply by the sum of electrostatic

(21) Tarakeshwar, P.; Lee, S. J.; Lee, J. Y.; Kim, K. S. *J. Chem. Phys.* **1998**, *108*, 7217.

and induction energies. Therefore, to increase this type of interaction, one needs to consider a system with highly electron-accepting moieties. On the other hand, the facially substituted aromatic system depends on not only the electron-donating ability responsible for the electrostatic energy but also the dispersion interaction and exchange repulsion. The dispersion energy, together with the exchange repulsion, augments the electrostatic energy in the facially substituted aromatic systems. In this regard, our work has refined the Hunter–Sanders work^{3a} on interactions involving axially and facially substituted aromatic systems. We discussed the stabilization/destabilization of the edge-to-face aromatic interactions by axial and facial substitutions and elucidated its origin. In particular, the difference between axial and facial substitutions is explained.

The systems with electron-accepting substituents (NO₂, CN, Br, Cl, F) favor the axial substituent conformation, while those with electron-donating substituents (NH₂, CH₃, OH) favor the facial substituent conformation. The substitution can strengthen the edge-to-face interaction, compared to the unsubstituted benzene dimer. The predicted maximum energy difference between substituted and unsubstituted systems is about 0.6 kcal/mol (1.2 kcal/mol for the disubstituted complex with an axial nitrobenzene and a facial aminobenzene). In the case of the axially substituted aromatic system, the Hammett's substituent constant is well correlated with the electron density at the para position, which is an important stabilizing factor. In the facially substituted aromatic system, the stability by substitution depends on not only the electron-donating ability but also the exchange

repulsion and dispersion interaction. Hammett-like constants σ'_c would describe the edge-to-face interactions at the center of substituted aromatic rings. In addition, we studied the edge-to-face interactions for the complex systems of an aromatic ring with another counterpart such as H₂, H₂O, HCl, and HF. In the latter three cases with large dipole moments, the change in the interaction energy by substitution is large. Understanding of the origin of these interaction energies would be useful for the design of novel supramolecular systems and novel molecular devices and for understanding the strength of T-shaped structures in biomolecular systems due to the edge-to-face interactions. In addition, the present study would be of importance in understanding electrophilic aromatic substitution reactions.

Acknowledgment. This work was supported by the KISTEP/CRI and BK21.

Note Added in Proof. During the long review process of this manuscript, a paper similar to our topic appeared recently.²² In contrast to its focus on the main component of the aromatic interactions, our work discusses the origin of energy differences between nine different substituents including nitro- and aminobenzenes as the extreme cases of the aromatic interactions, and we elucidate the origin of differences in aromatic interactions by facial and axial substitutions.

JA037454R

(22) Sinnokrot, M. S.; Sherrill, C. D. *J. Am. Chem. Soc.* **2004**, *126*, 7690.